

# The Capacity of Distributed PHY-Layer Sensor Networks

Mischa Dohler, *Member, IEEE*, Athanasios Gkelias, *Student Member, IEEE*, and A. Hamid Aghvami, *Fellow, IEEE*

**Abstract**—Sensor networks are comprised of nodes with minimal baseband and RF functionalities. In such networks, it is assumed that a source sensor communicates with a target sensor over a number of relaying sensors by utilising distributed low-complexity space-time encoding techniques, hence the resulting communication scenario is a generalised form of orthogonalised multiple-input-multiple-output (MIMO) channels. The contributions of this paper are the derivation of the Shannon capacity in terms of nats/s/Hz for such space-time encoded distributed communication scenarios. Closed form capacity expressions are derived for ergodic flat-fading Rayleigh and Nakagami channels, as well as the communication rate outage probabilities for aforementioned channels. It is shown that the distributed Alamouti scheme yields the best performance over ergodic channels. In the case of non-ergodic channels, the 3/4-rate sporadic space-time block code is shown to give optimum performance. Finally, Monte-Carlo simulations are used to assess the performance of distributed multistage sensor networks. It is shown that notable power savings can be achieved, compared to the traditional single link sensor networks.

*Index Terms*—

MIMO Systems, Distributed Information Systems, Sensor Networks

## I. INTRODUCTION

The concept of sensor networks is fairly new; therefore, little theoretical literature is available on them. Furthermore, there is no common consensus on the functionalities and inherent characteristics of sensor networks to date. Hence in this work, we assume that sensor networks have characteristics as described below.

**Characteristics.** The function of sensors is to sense certain features of their surroundings and pass this information to a unit which is capable of processing such data. The duty-cycle of sensors is rather low as is their data rate. The majority of the sensors are stationary allowing for stable routing paths from the source sensors to the target sensor or processing unit. A primary concern for a sensor is for it to consume as little power as possible as it has been envisaged that microscopic sensors will run on traditional batteries for months, if not for years. It is therefore a task of a sensor network designer to allow for data transmission with minimal power consumption. This requirement translates directly to a high capacity physical

layer, where a certain data rate is accomplished with as little power consumption as possible.

**Background.** Sensor networks are significantly different from traditional ad-hoc networks. Firstly, the number of sensor nodes in a sensor network can be several orders of magnitude higher than the number of nodes in an ad-hoc network. Moreover, sensor nodes are usually densely deployed, prone to failures and limited in power provision, computational complexity and memory. While most ad-hoc networks communicate on a point-to-point basis, sensor nodes mainly use a broadcast communication paradigm, and they may not have a global identification [1]. There is a wide range of applications in which such networks might be used, such as environmental monitoring and control, robotic control and guidance in automatic manufacturing environments, military surveillance, interactive toys, smart homes providing security, identification and personalisation, and health monitoring [2], [3]. Recently there has been a lot of interest in the building and deployment of sensor networks. Worth mentioning are the WINS [4] and SmartDust [5] projects which aim to integrate sensing, computing, and wireless communication capabilities into a small form factor to enable low-cost production of tiny sensor nodes in large numbers [6]. Concerning the Physical Layer of sensor networks, in [7] a physical layer driven approach to designing protocols, algorithms and applications that minimise the energy consumption of a sensor network systems is proposed. The energies consumed by  $M$ -ary and binary modulation are compared for their respective circuit power consumptions.  $M$ -ary modulation increases energy efficiency by reducing the transmission time of the device, but usually also increases the circuit complexity and power consumption. It has been observed [8] that diversity is most likely to be achieved in the frequency domain, since the static nature of the network and the single antenna on each sensor makes space or time diversity difficult to obtain. However, performance gains are observed if distributed space or time coding is deployed, as is demonstrated in this paper. In [3], methods are defined for the cooperative detection of targets by a distributed wireless sensor network, and for a cooperative transmission scheme of the results to a remote user. Some simple capacity calculations for the Gaussian case are also obtained, and finally a simple phase rotation scheme is described that allows a variable number of transmitters without a common phase reference to attain gains using simple non-coherent combining. Regarding the Medium Access Control (MAC), traditional wireless MAC protocols do not usually fit the requirements of a sensor network due to their unique resource constraints and application requirements [1].

Hence some of the most notable solutions for sensor

Manuscript received April 2, 2004; revised August 16, 2005; accepted August 19, 2005.

M. Dohler is with France Télécom R&D, 28 Chemin du Vieux Chêne, 38243 Meylan Cedex, France (phone: +33-4-7676-4514, fax: +33-4-7676-4450, email: Mischa.Dohler@francetelecom.com).

A. Gkelias and A.H. Aghvami are with King's College London, Centre for Telecommunications Research, 26-29 Drury Lane, London WC2B 5RL, UK (emails: {athansios.gkelias, hamid.aghvami}@kcl.ac.uk).

networks are the Self-Organizing Medium Access Control for Sensor Networks (SMACS) scheme and the Eavesdrop and Register (EAR) algorithms (both in [3]), the Hybrid TDMA/FDMA Based scheme in [7] and the CSMA-Based Medium Access in [10].

Since the main operating constraint for sensors is their available energy, any proposed solution for sensor networks must take energy considerations and energy savings into account. Power-aware and cost-aware metrics are the two main categories of metrics that have been devised to minimise power. Power-aware metrics aim to minimise the total power needed to route a message between two different locations, while cost-aware metrics look at methods to extend the nodes' battery lifetime [11]. In [2], a new power-aware routing protocol that is suitable for low energy and low bit rate networks is described. As employed in this protocol, the use of a simple probabilistic forwarding mechanism to send traffic on different routes helps to use the node resources more efficiently; indeed, simulation results shows an increase in network lifetime of up to 40% using this method. In [12], a dynamic power management (DMP) scheme is proposed, where the sensor node is turned off if no events occur. Such an event-driven power consumption is critical to maximise battery life. In [11], a number of power-aware (from a local point of view) routing protocols are evaluated. In these schemes, the routing protocol tries to make decisions using only information that is available from its neighbouring nodes.

Also relevant to the current work are [13]–[25] which achieve performance benefits due to cooperative transmission and reception. The therein performed analysis and proposed protocols demonstrate a diversity order equivalent to the total number or cooperating antenna elements.

**Assumptions.** In contrast to previously performed research, this work accomplishes considerable power savings in a sensor network by utilising distributed MIMO capacity techniques without cooperation between the nodes, hence minimising the signalling and traffic load in the network. Potential approaches here are to deploy Space-Time Block Codes (STBCs) [26]–[28], Space-Time Trellis Codes (STTCs) [29] or layered multiplexing (e.g. BLAST) [30]. Due to the severe power constraints, the simplest encoding strategy has been chosen, i.e. STBCs. The deployment of STBCs orthogonalises the MIMO channel and thus reduces it to an equivalent single-input-single-output (SISO) channel [31], [32]. That is a very desirable property, both from the complexity as well as analysis point of view.

For operational simplicity, it is assumed that each sensor is in possession of one antenna element only, and the transceiver is capable of operating either in time division multiple access (TDMA) mode or frequency division multiple access (FDMA) mode. In TDMA mode, each sensor receives data over the entire frequency band  $W$  and a frame duration  $T_1$ . After a possible processing, the data is re-transmitted over the entire frequency band  $W$  and in a frame duration  $T_2$ , during which time it is not capable of receiving any data. In FDMA mode, communication may occur continuously, but data is received in a fractional bandwidth  $W_1$  and re-transmitted in a fractional bandwidth  $W_2$ . Note that both of these bandwidths must not

overlap.

As will be explained more thoroughly in Section II, the limitation of having just one antenna element per sensor reduces the distributed communication scenario at most to a multiple-input-single-output (MISO) communication scenario. Also, since the sensors are spatially separated, no correlation will be observed, additionally simplifying analysis. Finally, to facilitate the analysis, synchronisation is assumed to be perfect.

**Contributions.** The contributions of this paper can be summarised as follows:

- A closed capacity expression for the orthogonalised ergodic MISO Rayleigh and Nakagami flat fading channels is derived, where the channel coefficients can have an arbitrary attenuation.
- A closed capacity outage probability expression for the orthogonalised ergodic MISO Rayleigh and Nakagami flat fading channels is derived, where the channel coefficients can have an arbitrary attenuation.
- The capacity behaviour of multistage distributed sensor networks is assessed and simulated. The performance is compared to the non-distributed case and appropriate conclusions are drawn.

**Paper Structure.** In Section II, the system model is described in detail. The principle of a distributed (sensor) network is explained, as is the encoding/decoding strategy at each sensor. In Section III, the closed form capacity expressions for orthogonalised ergodic MISO channels obeying Rayleigh and Nakagami fading distributions is derived. In Section IV, the respective outage probabilities are derived in closed form. The end-to-end ergodic capacity and capacity outage probability is studied in Section V. Here, a source sensor delivers information to a target sensor via a plurality of relaying sensors. Finally, conclusions are drawn in Section VI.

## II. SYSTEM MODEL

### A. Principle of Distributed Sensor Network

Given is a source sensor (s-S) which intends to deliver information to a target sensor (t-S) or processing unit via a given number of distributed relaying sensors (r-Ss), as depicted in Figure 1. The s-S sends its information to a group of spatially adjacent r-Ss, which form the first tier r-Ss. Since no cooperation between the nodes is allowed, the end-to-end diversity order is limited to the weakest relaying stage which is the first stage. The achieved diversity order of 1 requires that the first tier sensor nodes is spatially close to the s-S so as to minimise the power spent to reach the first tier.

The signal stream from the s-S is reached by the first tier r-Ss which space-time encode the data stream, i.e. each r-S transmits only a spatial fraction of the space-time code word such that the total output from the first tier r-Ss comprises a MISO transmission. Since the MISO channel achieves a higher capacity and lower outage probability [39], the distance between the first and second relaying tier can be considerably larger than from the s-S to the first relaying tier or, alternatively, the transmission power can be reduced.

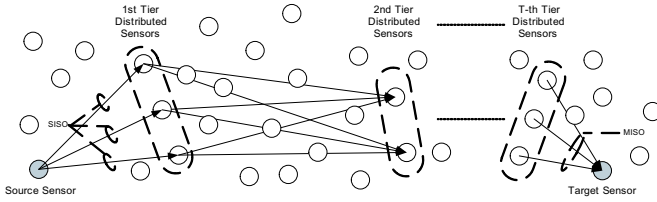


Fig. 1. Distributed sensor network, where a source sensor communicates with a target sensor via a number of sensor tiers, each of which is formed of distributed relaying sensors.

The second tier r-Ss receives the data stream, de-codes it, re-encodes and re-transmits it to the third tier r-Ss in the same manner as described above. This process is continued until the t-S or the processing unit is reached. Note that it is not the aim of this paper to deal with the optimum data routing path through the distributed sensor network; it is also assumed that the tiers of r-Ss are already formed and the sensors know about which spatial fraction of a space-time code word they have to (re-) transmit. The distributed encoding process is described in more detail as follows, where a FDMA-based relaying system with  $T$  relaying sensor tiers is assumed.

**Source Sensor.** The s-S Gray-maps  $b_0$  source information bits onto symbol  $x$  by utilising a  $M_0$ -PSK (or  $M_0$ -QAM) signal constellation, where  $b_0 = \log_2 M_0$ . The data stream is transmitted on frequency band  $W_0$  with power  $S_0$ .

**First Tier Relaying Sensors.** The first tier r-Ss receive the data on frequency band  $W_0$ , detect it, space-time encode it and transmit it simultaneously on frequency band  $W_1$  with a total power  $S_1$ . Each r-S Gray-maps  $K_1 b_1$  bits onto symbols  $x_1, x_2, \dots, x_K$  by utilising an  $M_1$ -PSK (or  $M_1$ -QAM) signal constellation, where  $b_1 = \log_2 M_1$  and  $K_1$  is the number of symbols per space-time encoding.

The  $\{x_k\}_{k=1}^{K_1}$  are encoded with an orthogonal space-time coding matrix  $\mathcal{G}_1$  of size  $p_1 \times d_1$ , where  $p_1$  is the number of symbol durations required to transmit the space-time code word, and  $d_1$  is the number of distributed r-Ss (and therefore equivalent to the number of transmit antennas). At each time instant  $t$ , the encoded symbol  $c_{t,i}$  with  $t = 1, \dots, p_1$  and  $i = 1, \dots, d_1$  is transmitted simultaneously from the  $i^{\text{th}}$  distributed r-S. Clearly, the rate of the first tier space-time block code is  $R_1 = K_1/p_1$ .

**$T^{\text{th}}$  Tier Relaying Sensors.** The  $T^{\text{th}}$  tier r-Ss receive data on frequency band  $W_{T-1}$ , space-time decode it, space-time re-encode it and re-transmit it on frequency band  $W_T$  with a total power  $S_T$ . The encoding procedure is the same as described above, where the rate of the STBC is  $R_T$ .

**Target Sensor.** The t-S receives the data on frequency band  $W_T$ , space-time decodes it and performs the final detection. If the s-S deploys a channel code, e.g. a simple trellis code, then the t-S performs the equivalent channel decoding to boost performance.

Each relaying sensor tier clearly may use a different signal constellation and STBC. It is only of importance that the consecutive tier has knowledge of the transmission parameters of the previous tier.

## B. The Equivalent SISO Model

To improve readability, superscripts related to the respective relaying tier are omitted here. Given is one relaying stage with  $n_T$  distributed transmit sensors and  $n_R$  distributed receive sensors. Because sensors of the same tier do not communicate among each other, there are  $n_R$  MISO channels with  $n_T$  transmit antennas. Also, because of the spatial separation between sensors, the rather low data rates generated by sensor networks, and the low mobility prevailing in indoor environments, the channel coefficients are assumed to be independent, frequency flat and quasi-static. Without loss of generality, only one MISO channel from the  $n_r$  available is considered here. The channel matrix thus reduces to a  $1 \times n_T$  channel vector  $\mathbf{h}$  and it is defined as

$$\mathbf{h} \triangleq (h_1, \dots, h_{n_T}) \quad (1)$$

where  $h_i$ ,  $i = (1, \dots, n_T)$  denotes the channel gain from the  $i^{\text{th}}$  transmit sensor to the receive sensor. The use of orthogonal space-time block codes is known to decouple the MIMO (here MISO) channel into parallel SISO channels [31]-[33]. This property is henceforth referred to as an orthogonalisation of the MIMO (here MISO) channel. This advantageous property may come at a loss in transmission rate  $R$ , which is defined as

$$R \triangleq \frac{K}{p} \quad (2)$$

where  $K$  is the number of symbols per space-time encoding and  $p$  is the number of symbol durations required to transmit the space-time code word [33]. For fixed channel realisations  $\mathbf{h}$ , the normalised capacity in nats/s/Hz over such orthogonalised MISO channel can be expressed as [33]

$$C = R \log \left( 1 + \frac{1}{R} \frac{\|\mathbf{h}\|^2 S}{n_T N} \right) \quad (3)$$

where  $S$  is the average transmitted power and  $N$  the noise power at the receiver.  $\|\mathbf{h}\|$  denotes the Frobenius norm of  $\mathbf{h}$ , the square of which is given as

$$\|\mathbf{h}\|^2 = \sum_{i=1}^{n_T} |h_i|^2 = \text{tr}(\mathbf{h}\mathbf{h}^H) \quad (4)$$

where the superscript  $H$  denotes the Hermitian and  $\text{tr}(\cdot)$  is the trace operator. If the channel realisations  $\mathbf{h}$  are random, then the ergodic channel capacity is obtained by averaging over all channel conditions  $\|\mathbf{h}\|^2 \triangleq \lambda$ , i.e.

$$C = E_\lambda \left\{ R \log \left( 1 + \frac{1}{R} \frac{\lambda S}{n_T N} \right) \right\} \quad (5)$$

$$= \int_0^\infty R \log \left( 1 + \frac{1}{R} \frac{\lambda S}{n_T N} \right) f_\lambda(\lambda) d\lambda \quad (6)$$

where  $E_\lambda\{\cdot\}$  denotes the expectation with respect to  $\lambda$  with a probability density function (pdf) of  $f_\lambda(\lambda)$ .

Finally, the average signal-to-noise ratio (SNR) per symbol at detection can be expressed as [33]

$$\bar{\gamma} = \frac{1}{R} \frac{E\{\|\mathbf{h}\|^2\} S}{n_T N} \quad (7)$$

Defining  $E\{h_i h_i^*\} \triangleq \alpha_i^2$ ,  $i = (1, \dots, n_T)$ , where the superscript \* denotes the complex conjugate, then (7) can be rewritten as

$$\bar{\gamma} = \frac{1}{R} \frac{\sum_{i=1}^{n_T} \alpha_i^2 S}{n_T N} \quad (8)$$

which will be useful for subsequent analysis.

### III. ERGODIC CAPACITY OF ORTHOGONALISED DISTRIBUTED MISO CHANNELS

#### A. The Capacity Integral

A closed form expression for the Shannon capacity over ergodic Rayleigh flat fading MIMO channels is presented here. It is utilised later in the paper to compare the capacity of a generic MISO channel with the capacity of an orthogonalised MISO channel. This derivation of the closed form expression requires knowledge of the solution of the capacity integral, which is frequently encountered in calculating MIMO or MISO capacities.

The capacity  $C$  in nats/s/Hz of a normalised ergodic Rayleigh flat fading MIMO channel with  $n_T$  transmit and  $n_R$  receive antennas constrained by power  $S$  was elegantly derived by Telatar [39] as

$$C = \int_0^\infty \log \left( 1 + \frac{\lambda S}{n_T N} \right) \cdot \sum_{k=0}^{m-1} \frac{k!}{(k+n-m)!} [L_k^{n-m}(\lambda)]^2 \lambda^{n-m} e^{-\lambda} d\lambda \quad (9)$$

where  $N$  is the received noise power,  $m = \min\{n_R, n_T\}$ ,  $n = \max\{n_R, n_T\}$  and  $L_k^{n-m}(\lambda)$  is the associated Laguerre polynomial of order  $k$ . This can be conveniently expressed as

$$C = E_\lambda \left\{ m \log \left( 1 + \frac{\lambda S}{n_T N} \right) \right\} \quad (10)$$

with

$$f_\lambda(\lambda) = \frac{1}{m} \sum_{k=0}^{m-1} \frac{k!}{(k+n-m)!} [L_k^{n-m}(\lambda)]^2 \lambda^{n-m} e^{-\lambda} \quad (11)$$

where  $f_\lambda(\lambda)$  is the pdf of an unordered eigenvalue  $\lambda$  [39]. A closed form expression in terms of finite sums for the capacity given in (9) was derived in [37] and is given as

$$C = \sum_{k=0}^{m-1} \frac{k!}{(k+d)!} \left[ \sum_{l=0}^k A_l^2(k, d) \hat{C}_{2l+d}(\tau) + \sum_{l_1=0}^k \sum_{l_2=0, l_2 \neq l_1}^k (-1)^{l_1+l_2} A_{l_1}(k, d) A_{l_2}(k, d) \hat{C}_{l_1+l_2+d}(\tau) \right] \quad (12)$$

where  $d \triangleq n - m$ ,  $A_l(k, d) \triangleq (k+d)! / [(k-l)! (d+l)! l!]$  and  $\tau \triangleq \frac{1}{n_T} \frac{S}{N}$ .  $\hat{C}_\zeta(\tau)$  is defined as

$$\hat{C}_\zeta(\tau) \triangleq \int_0^\infty \log(1 + \tau x) x^\zeta e^{-x} dx. \quad (13)$$

Because of its frequent occurrence, this expression is henceforth referred to as the **capacity integral**. The solution to the

capacity integral is given as [37]

$$\hat{C}_\zeta(\tau) = \sum_{\mu=0}^{\zeta} \frac{\zeta!}{(\zeta-\mu)!} \left[ (-1)^{\zeta-\mu-1} (1/\tau)^{\zeta-\mu} e^{1/\tau} \text{Ei}(-1/\tau) + \sum_{k=1}^{\zeta-\mu} (k-1)! (-1/\tau)^{\zeta-\mu-k} \right] \quad (14)$$

where  $\text{Ei}(y) \equiv \int_{-\infty}^y \frac{e^t}{t} dt$  is the exponential integral. Hence the capacity of a generic MISO channel can be expressed in closed form as

$$C = \frac{1}{\Gamma(n_T)} \cdot \hat{C}_{n_T-1} \left( \frac{1}{n_T} \frac{S}{N} \right), \quad (15)$$

where  $\Gamma(x)$  is the complete Gamma function.

#### B. Orthogonalised MISO - Ergodic Capacity - Rayleigh Fading

**Equal Channel Gains.** If all channel gains are equal then  $E\{h_1 h_1^*\} = \dots = E\{h_{n_T} h_{n_T}^*\} \equiv \alpha^2$ . Clearly,  $\mathbf{h} \mathbf{h}^H$  has rank one; therefore, the capacity determining eigenvalue  $\lambda$  of  $\mathbf{h} \mathbf{h}^H$  [39] is equal to  $\mathbf{h} \mathbf{h}^H$ , i.e.  $\lambda = \mathbf{h} \mathbf{h}^H = \|\mathbf{h}\|^2$ . Because  $\|\mathbf{h}\|^2$  has a central chi-square distribution with  $2n_T$  degrees of freedom and mean  $E\{\lambda\} = n_T \alpha^2$ , the pdf of  $\lambda$  can be expressed as [38]

$$f_\lambda(\lambda) = \frac{1}{\Gamma(n_T)} \frac{\lambda^{n_T-1}}{(\alpha^2)^{n_T}} e^{-\lambda/\alpha^2} \quad (16)$$

With reference to (6) and some changes in variables, the capacity of the orthogonalised MISO channel can be expressed in closed form as

$$C = \frac{R}{\Gamma(n_T)} \int_0^\infty \log \left( 1 + \lambda \frac{1}{R} \frac{\alpha^2 S}{n_T N} \right) \lambda^{n_T-1} e^{-\lambda} d\lambda \quad (17)$$

$$= \frac{R}{\Gamma(n_T)} \cdot \hat{C}_{n_T-1} \left( \frac{1}{R} \frac{\alpha^2 S}{n_T N} \right) = \frac{R}{\Gamma(n_T)} \cdot \hat{C}_{n_T-1} \left( \frac{\bar{\gamma}}{n_T} \right) \quad (18)$$

where  $\bar{\gamma} = \frac{\alpha^2 S}{R N}$ .

Figure 2 depicts the normalised Shannon capacity in nats/s/Hz versus  $S/N$  in dB for various MISO system configurations and  $\alpha^2 = 1$ . Depicted are the following cases: (1)  $n_T = 1$  (SISO), (2)  $n_T = 2$  (Alamouti), (3)  $n_T = 3$  (3/4-Rate), (4)  $n_T = 4$  (3/4-Rate), (5)  $n_T = 3$  (Half-Rate), (6)  $n_T = 4$  (Half-Rate), (7)  $n_T = 3$  (generic MISO), (8)  $n_T = 4$  (generic MISO).

It can be observed that capacity increases for the generic MISO channels with an increasing number of transmit antennas. The same holds for the full-rate Alamouti STBC, which yields an asymptotic capacity gain of 0.3nats/s/Hz or an equivalent power savings of 1.25dB.

Interestingly, however, if the MISO channel is orthogonalised with the aid of half-rate or even 3/4-rate orthogonal STBCs, no capacity benefits can be observed. Note that the STBCs only orthogonalise the MISO channel; however, they do not give any coding gain. Therefore, if these bounds were to be approached, an outer channel code would have to be developed.

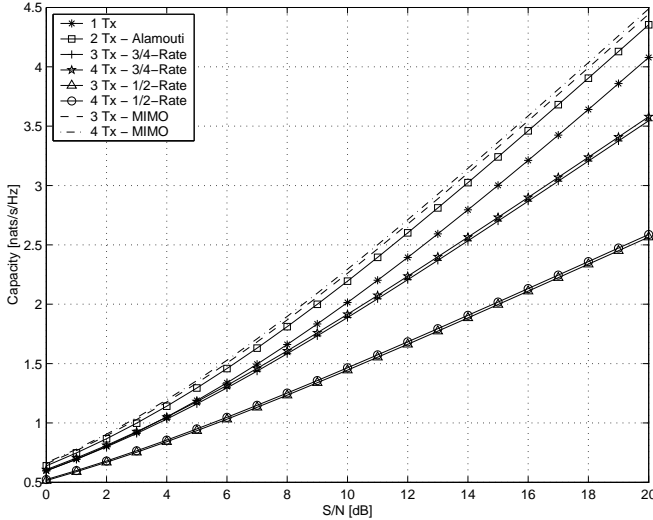


Fig. 2. Normalised Shannon Capacity in nats/s/Hz versus  $S/N$  in dB for various STBCs over a MISO Rayleigh channel with equal channel gains;  $\alpha^2 = 1$ .

**Unequal Channel Gains.** The capacity expression in closed form for the unequal channel gains is derived utilising the moment generating function (MGF), which is defined as  $\phi_\lambda(s) \triangleq \int_0^\infty e^{-s\lambda} f_\lambda(\lambda) d\lambda$  [40]. The MGF  $\phi_{\lambda_i}(s)$  of the  $i^{\text{th}}$  MISO Rayleigh channel with instantaneous power  $\lambda_i \triangleq h_i h_i^*$  (and average power  $\alpha_i^2 \triangleq E\{h_i h_i^*\}$ ) can hence be derived as

$$\phi_{\lambda_i}(s) = \frac{1}{1 - s\alpha_i^2} \quad (19)$$

The addition of the random channel gains according to (4) results in the convolution of their pdfs, which equates to the product of their MGFs. Therefore, the MGF of the MISO channel can be expressed as

$$\phi_\lambda(s) = \prod_{i=1}^{n_T} \phi_{\lambda_i}(s) = \frac{1}{1 - s\alpha_1^2} \cdot \frac{1}{1 - s\alpha_2^2} \cdots \frac{1}{1 - s\alpha_{n_T}^2} \quad (20)$$

Resolving (20) into its partial fractions, one can write

$$\phi_\lambda(s) = \sum_{i=1}^{n_T} K_i \phi_{\lambda_i}(s) \quad (21)$$

where the constants - poles of the MGF - are obtained by solving the set of linear equations, the solution to which is [44]

$$K_i = \prod_{i'=1, i' \neq i}^{n_T} \frac{\alpha_i^2}{\alpha_i^2 - \alpha_{i'}^2} \quad (22)$$

The linearity of the inverse of the MGF allows therefore writing for the pdf of the eigenvalue  $\lambda = \|\mathbf{h}\|^2$

$$f_\lambda(\lambda) = \sum_{i=1}^{n_T} K_i \cdot \frac{1}{\alpha_i^2} e^{-\lambda/\alpha_i^2} \quad (23)$$

The capacity of the MISO link with unequal channel coefficients can finally be expressed in closed form as

$$C = R \sum_{i=1}^{n_T} K_i \cdot \hat{C}_0 \left( \frac{1}{R} \frac{\alpha_i^2}{n_T} \frac{S}{N} \right) = R \sum_{i=1}^{n_T} K_i \cdot \hat{C}_0(\bar{\gamma}_i). \quad (24)$$

Figure 3 depicts the normalised Shannon capacity in nats/s/Hz versus  $S/N$  in dB for the distributed Alamouti scheme. In the case of equal channel coefficients, the expectation of the square of the Frobenius norm of the normalised channel coefficients would yield  $n_T$ ; here  $n_T = 2$ . For this reason, the power of the unequal channel coefficients is chosen such that  $\alpha_1^2 + \alpha_2^2 \equiv 2$ . Chosen was the particular case where  $\alpha_1^2 : \alpha_2^2 = 2 : 1$ , i.e.  $\alpha_1^2 = 4/3$  and  $\alpha_2^2 = 2/3$ . Depicted are the cases where only channel with power  $\alpha_1^2$  is utilised, and where only channel with power  $\alpha_2^2$  is utilised, and where the distributed Alamouti STBC is utilised. The latter is corroborated by numerical simulations.

Clearly, the loss in capacity of the distributed communication scenario is negligible compared to the case where communication happens through the stronger single link. However, a considerable capacity loss can be observed when the weaker single link is utilised. Therefore, when only a single link is deployed then shadowing may severely degrade the link capacity; whereas when a distributed encoding is chosen then the capacity is fairly robust to attenuations in either link. A quantification of the performance gains when independent shadowing dominates the communication system is postponed to Section V.

Figure 4 depicts the normalised Shannon capacity in nats/s/Hz versus  $S/N$  in dB for the distributed 3/4-rate STBC scheme. Here, the ratio between the channel coefficients was chosen such that  $\alpha_1^2 : \alpha_2^2 : \alpha_3^2 = 4 : 2 : 1$ , i.e.  $\alpha_1^2 = 12/7$ ,  $\alpha_2^2 = 6/7$  and  $\alpha_3^2 = 3/7$ . Again, severe capacity losses can be observed when communication happens only over the weaker single links; however, the distributed communication scenario offers a robust capacity. Note, however, that the absolute ergodic capacity of the 3/4-rate STBC is inferior to the ergodic capacity of the full-rate Alamouti scheme.

Figure 5 depicts the normalised Shannon capacity in nats/s/Hz versus the normalised power in the first link  $\alpha_1^2$  for the distributed Alamouti scheme with  $S/N = 10$  dB.

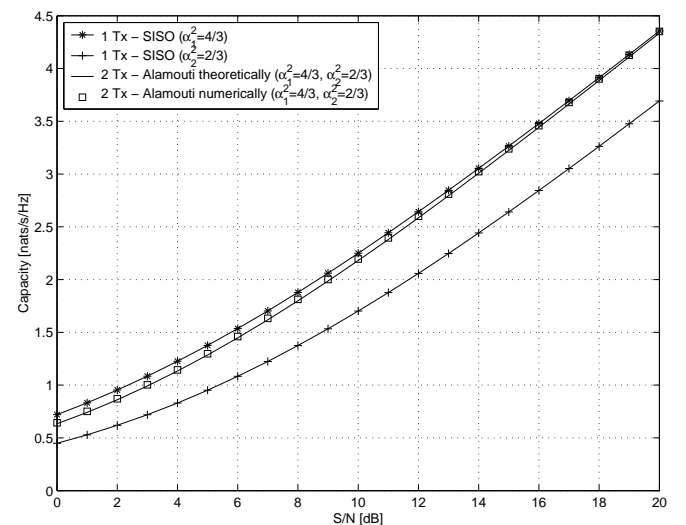


Fig. 3. Normalised Shannon Capacity in nats/s/Hz versus  $S/N$  in dB for the distributed Alamouti STBC over a MISO Rayleigh channel with unequal channel gains;  $\alpha_1^2 = 4/3$  &  $\alpha_2^2 = 2/3$ .

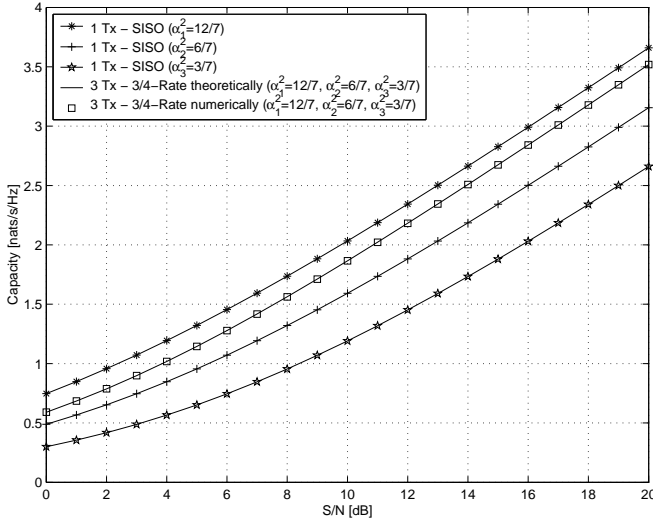


Fig. 4. Normalised Shannon Capacity in nats/s/Hz versus  $S/N$  in dB for the distributed 3/4-rate sporadic STBC over a MISO Rayleigh channel with unequal channel gains;  $\alpha_1^2 = 12/7$  &  $\alpha_2^2 = 6/7$  and  $\alpha_3^2 = 3/7$ .

Furthermore, depicted are the cases where communication happens only over either of the single links, where  $\alpha_2^2 = 2 - \alpha_1^2$ . The distributed Alamouti scheme outperforms even the strongest link for  $0.8 < \alpha_1^2 < 1.2$ . Notably, the capacity of the distributed scheme is much less dependent on the power of the individual links than in the case of the single link schemes. Similar observations can be made for higher order STBCs. This corroborates the advantage of a distributed sensor network where channel conditions are not known a priori and feedback is limited.

**Generic Channel Gains.** Generally, the channel gains can be different where some gains are repeated. In this case, the MGF of the eigenvalue  $\lambda$  of the MISO channel can be

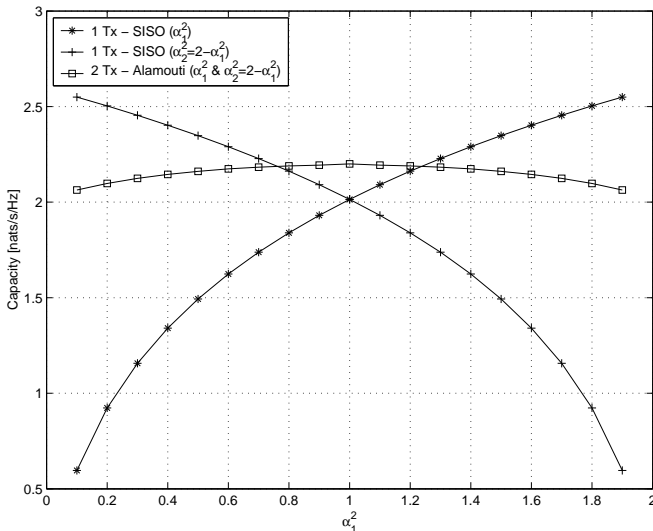


Fig. 5. Normalised Shannon capacity in nats/s/Hz versus the normalised power in the first link  $\alpha_1^2$  for the distributed Alamouti scheme over a MISO Rayleigh channel;  $S/N = 10$ dB.

expressed as

$$\begin{aligned} \phi_\lambda(s) &= \prod_{i=1}^{n_T} \phi_{\lambda_i}(s) \\ &= \frac{1}{(1 - s\alpha_1^2)^{\nu_1}} \cdot \frac{1}{(1 - s\alpha_2^2)^{\nu_2}} \cdots \frac{1}{(1 - s\alpha_g^2)^{\nu_g}} \end{aligned} \quad (25)$$

where  $g$  is the number of different channel coefficients,  $\sum_{i=1}^g \nu_i \equiv n_T$  and  $\alpha_i^2, i = (1, \dots, g)$ , the distinct but possibly repeated average channel gains. Resolving (25) into its partial fractions with repeated roots yields

$$\phi_\lambda(s) = \sum_{i=1}^g \sum_{j=1}^{\nu_i} K_{i,j} \phi_{\lambda_i}^j(s) \quad (26)$$

In the appendix, the coefficients  $K_{i,j}$  are derived as

$$\begin{aligned} K_{i,j} &= \frac{1}{(\nu_i - j)! (-\alpha_i^2)^{\nu_i - j}} \cdot \\ &\frac{\partial^{\nu_i - j}}{\partial s^{\nu_i - j}} \left[ \prod_{i'=1, i' \neq i}^g \frac{1}{(1 - s\alpha_{i'}^2)^{\nu_{i'}}} \right]_{s=1/\alpha_i^2} \end{aligned} \quad (27)$$

This allows one to express the  $f_\lambda(\lambda)$  in closed form as

$$f_\lambda(\lambda) = \sum_{i=1}^g \sum_{j=1}^{\nu_i} K_{i,j} \cdot \frac{\lambda^{j-1}}{\Gamma(j) \cdot (\alpha_i^2)^j} e^{-\lambda/\alpha_i^2} \quad (28)$$

The capacity of the generic MISO link with can now be expressed in closed form as

$$C = R \sum_{i=1}^g \sum_{j=1}^{\nu_i} K_{i,j} \cdot \hat{C}_{j-1} \left( \frac{1}{R} \frac{\alpha_i^2}{n_T} \frac{S}{N} \right) \quad (29)$$

$$= R \sum_{i=1}^g \sum_{j=1}^{\nu_i} K_{i,j} \cdot \hat{C}_{j-1}(\bar{\gamma}_i) \quad (30)$$

### C. Orthogonalised MISO - Ergodic Capacity - Nakagami Fading

**Equal Channel Gains.** The indoor fading distribution was often found to obey a Nakagami distribution [40], which is thus particularly important for indoor sensor networks. The pdf of the instantaneous power  $\lambda_i$  (and average power  $\alpha_i^2$ ) of the  $i^{\text{th}}$  Nakagami channel can be expressed as [40]

$$f_{\lambda_i}(\lambda_i) = \frac{m_i^{m_i} \lambda_i^{m_i-1}}{(\alpha_i^2)^{m_i} \Gamma(m_i)} e^{-m_i \lambda_i / \alpha_i^2} \quad (31)$$

where  $m_i$  is the Nakagami- $m$  fading parameter of the  $i^{\text{th}}$  channel ranging from  $m_i = (1/2, \infty)$ . Note that for  $m_i = 1$ , the Nakagami distribution turns into a Rayleigh distribution. Furthermore, the Ricean distribution with parameter  $K$  can be closely approximated with the Nakagami- $m$  distribution, where  $m = \frac{(1+K)^2}{1+2K}$  [40].

The MGF of the instantaneous power of the  $i^{\text{th}}$  Nakagami channel can be expressed as [40]

$$\phi_{\lambda_i}(s) = \frac{1}{(1 - s \frac{\alpha_i^2}{m_i})^{m_i}} \quad (32)$$

For  $n_T$  identically distributed Nakagami fading channels, i.e.  $\alpha_1^2 = \dots = \alpha_{n_T}^2 = \alpha^2$  and  $m_1 = \dots = m_{n_T} = m$ , the MGF of the eigenvalue  $\lambda = \|\mathbf{h}\|^2$  is therefore given as

$$\phi_\lambda(s) = \left[ \frac{1}{\left(1 - s \frac{\alpha^2}{m}\right)^m} \right]^{n_T} \quad (33)$$

the inverse of which leads to the desired pdf of the eigenvalue of a Nakagami distributed MISO channel

$$f_\lambda(\lambda) = \frac{m^{mn_T} \lambda^{mn_T-1}}{(\alpha^2)^{mn_T} \Gamma(mn_T)} e^{-m\lambda/\alpha^2} \quad (34)$$

The capacity for  $m \in \mathbb{N}$  is solvable in closed form as

$$C = \frac{R}{\Gamma(mn_T)} \cdot \hat{C}_{mn_T-1} \left( \frac{1}{R} \frac{\alpha^2}{mn_T} \frac{S}{N} \right) \quad (35)$$

$$= \frac{R}{\Gamma(mn_T)} \cdot \hat{C}_{mn_T-1} \left( \frac{\bar{\gamma}}{mn_T} \right) \quad (36)$$

where  $\bar{\gamma} = \frac{\alpha^2}{R} \frac{S}{N}$ . Note that if  $m \in \mathbb{R}$  then  $m$  should be replaced by  $\lfloor m \rfloor$  to obtain a lower bound, i.e. the capacity which is at least achieved by the ergodic Nakagami MISO channel.

Figure 6 depicts the normalised Shannon capacity in nats/s/Hz versus  $S/N$  in dB for various MISO system configurations and  $\alpha^2 = 1$  over a Nakagami channel. Depicted are the following cases: (1)  $n_T = 1$  (SISO) with  $m = 1$  (Rayleigh), (2)  $n_T = 1$  (SISO) with  $m = 10$  (strong LOS), (3)  $n_T = 2$  (Alamouti) with  $m = 1$  (Rayleigh), (4)  $n_T = 2$  (Alamouti) with  $m = 10$  (strong LOS), (5) Gaussian channel for comparison. Clearly, for  $m = 10$ , i.e. a strong LOS communication scenario, capacity reaches Gaussian performance. This is independent from the number of transmit antennas as the fading channel exhibits very little fluctuations for high  $m$ .

Figure 7 depicts the normalised Shannon capacity in nats/s/Hz versus the Nakagami  $m$  fading factor for various MISO system configurations;  $S/N = 10$  dB and  $\alpha^2 = 1$ . The Nakagami  $m$  fading factor is varied from  $m = 1$  (Rayleigh)

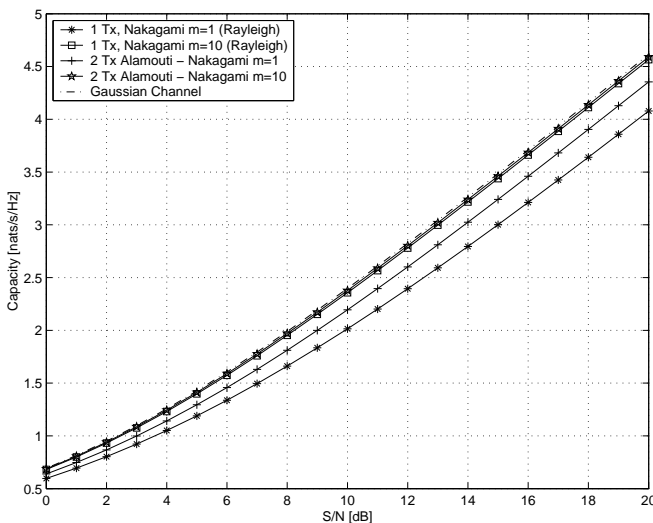


Fig. 6. Normalised Shannon capacity in nats/s/Hz versus  $S/N$  in dB for the single link case and the Alamouti scheme over an identically distributed MISO Nakagami channel with varying  $m$ -factor;  $\alpha^2 = 1$ .

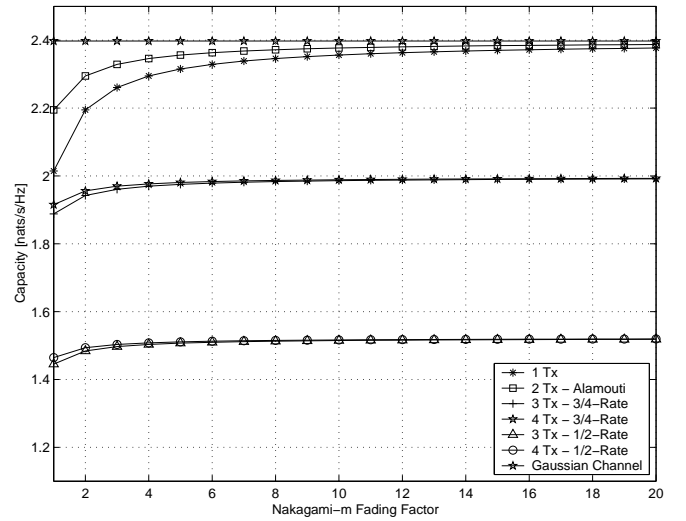


Fig. 7. Normalised Shannon capacity in nats/s/Hz versus the Nakagami  $m$  fading factor for various MISO system configurations;  $S/N = 10$  dB and  $\alpha^2 = 1$ .

to  $m = 20$  (very strong LOS). Compared are the following scenarios: (1)  $n_T = 1$  (SISO), (2)  $n_T = 2$  (Alamouti), (3)  $n_T = 3$  (3/4-Rate), (4)  $n_T = 4$  (3/4-Rate), (5)  $n_T = 3$  (Half-Rate), (6)  $n_T = 4$  (Half-Rate), (7) Gaussian channel for comparison.

Interestingly, capacity is rather independent of  $m$  for the 3/4 and 1/2 rate STBCs; however, generally inferior to the capacity of the full-rate STBCs. Their low dependency is explained with the high diversity already obtained from the 3 and 4 transmit antennas. Their low performance comes from the rate loss due to  $R < 1$ . Furthermore, the Alamouti STBC converges to the Gaussian capacity faster than the one transmit antenna case does. It is worth noting that, as long as ergodic Shannon capacity is the system performance measure, distributed communication scenarios under LOS conditions do not yield any significant capacity benefit. However, with unequal link attenuations due to shadowing, the distributed case yields significant benefits as demonstrated below.

**Unequal Channel Gains.** Here, the same procedure as for the Rayleigh fading case is repeated. The MGF  $\phi_\lambda(s)$  of the eigenvalue  $\lambda = \|\mathbf{h}\|^2$  of the MISO channel with  $n_T$  transmit antennas can be expressed as

$$\begin{aligned} \phi_\lambda(s) &= \prod_{i=1}^{n_T} \phi_{\lambda_i}(s) \\ &= \frac{1}{\left(1 - s \frac{\alpha_1^2}{m_1}\right)^{m_1}} \cdot \frac{1}{\left(1 - s \frac{\alpha_2^2}{m_2}\right)^{m_2}} \cdots \frac{1}{\left(1 - s \frac{\alpha_{n_T}^2}{m_{n_T}}\right)^{m_{n_T}}} \end{aligned} \quad (37)$$

where  $m_i$  is the Nakagami fading parameter of the  $i^{\text{th}}$  link. Repeating the procedure of the MISO Rayleigh fading case, finally yields for the capacity

$$C = R \sum_{i=1}^{n_T} \sum_{j=1}^{m_i} K_{i,j} \cdot \frac{1}{\Gamma(j)} \hat{C}_{j-1} \left( \frac{1}{R} \frac{\alpha_i^2}{jn_T} \frac{S}{N} \right) \quad (38)$$

$$= R \sum_{i=1}^{n_T} \sum_{j=1}^{m_i} K_{i,j} \cdot \frac{1}{\Gamma(j)} \hat{C}_{j-1} \left( \frac{\bar{\gamma}_i}{j} \right) \quad (39)$$

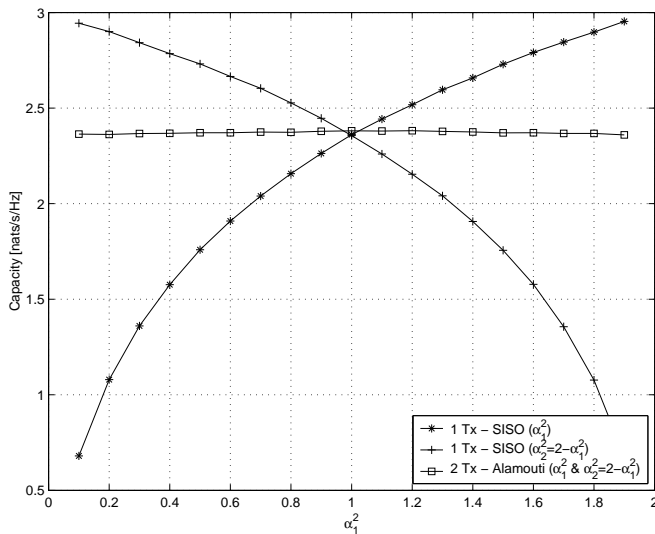


Fig. 8. Normalised Shannon capacity in nats/s/Hz versus the normalised power in the first link  $\alpha_1^2$  for the distributed Alamouti scheme over a MISO Nakagami channel;  $S/N = 10\text{dB}$  and  $m = 10$ .

where the coefficients  $K_{i,j}$  are now found by performing partial fractions on (37).

Figure 8 depicts the normalised Shannon capacity in nats/s/Hz versus the normalised power in the first link  $\alpha_1^2$  over a Nakagami fading channel for the distributed Alamouti scheme;  $S/N = 10\text{dB}$  and  $m = 10$ . Again, depicted are the cases where communication happens only over either of the single links, where  $\alpha_2^2 = 2 - \alpha_1^2$ . Clearly, the region where the distributed Alamouti scheme outperforms the stronger link has reduced to a single point for  $\alpha_1^2 = 1$ . Furthermore, the capacity of the distributed scenario is up to 15% lower than of the stronger single link case. However, the capacity of the distributed scenario is virtually independent of the fading coefficients. Therefore, if the sensors are potentially shadowed, then the distributed communication scenario offers a significant performance stability.

**Generic Channel Gains.** The case of generic channel coefficients is similarly obtained as for the Rayleigh channel and is thus omitted here.

#### IV. OUTAGE CAPACITY OF ORTHOGONALISED DISTRIBUTED MISO CHANNELS

Given each realisation of the MISO channel  $\mathbf{h}$  to be memoryless or ergodic, the maximum mutual information is referred to as capacity [39]. To achieve this capacity, codebook entries of infinite length and given capacity-maximising covariance have to be generated. The capacity of such channels has been dealt with in the previous section. Here, the case of non-ergodic channels is analysed; in particular, the case where the channel realisations are randomly fixed at the beginning of the transmission and kept constant over the infinite transmission duration. The requirement on the infinite length of the codebook entries can be loosened; the performance can then be quantified with the aid of the random coding theory [39]. It can be shown that for increasing code length, the upper capacity bound is reached exponentially. Practically,

this implies that the codes deployed by the sensors can be of finite (and comparably short) length without losing too much in performance.

Since the channel realisation  $\mathbf{h}$  is chosen randomly and kept constant over the codeword transmission, there is a non-zero probability that a given transmission rate  $R_C$  cannot be supported by the channel [39]. However, the probability that a certain communication rate  $R_C$  can be supported by a channel  $\mathbf{h}$  with average codeword power  $S$  can be gauged, and is referred to as the outage probability  $P_{out}(R_C, S, \mathbf{h})$ . It is therefore the aim to maximise  $P_{out}$  for a given channel, average codeword power and required communication rate. That can be achieved by choosing suitable codewords  $\mathbf{x}$  with a given covariance matrix  $Q = E\{\mathbf{x}\mathbf{x}^H\}$ , so that  $P_{out}(R_C, S, \mathbf{h})$  equates  $\inf \{ \text{probability}(\log \det(\mathbf{I} + \mathbf{h}\mathbf{Q}\mathbf{h}^H) < R_C) \}$  subject to  $Q : Q > 0, \text{tr}(Q) \leq S$  [39], where  $\mathbf{I}$  is the unit matrix. Furthermore, in [39] (Example 6) it has been shown that if the rank of  $\mathbf{h}\mathbf{h}^H$  is one then  $Q = S$  is optimal. That allows one to derive closed form expressions for the outage probabilities for various channels by evaluating the channel outage probability induced by the randomness of the instantaneous channel power, here  $\mathbf{h}\mathbf{h}^H = \|\mathbf{h}\|^2 = \lambda$ , with the appropriate bounds:

$$P_{out}(R_C, S, \mathbf{h}) = \int_0^{\lambda_{R_C}} f_\lambda(\lambda) d\lambda \quad (40)$$

where, with reference to (5),  $\lambda_{R_C} = (e^{R_C/R} - 1) \left[ \frac{1}{R} \frac{1}{n_T} \frac{S}{N} \right]^{-1}$ .

#### A. Orthogonalised MISO - Outage Capacity - Rayleigh Fading

**Equal Channel Gains.** Computing (40) for the Rayleigh fading channel with the pdf given by (16), one obtains

$$P_{out}(R_C, S, \mathbf{h}) = \frac{1}{\Gamma(n_T)} \gamma \left( n_T, \frac{e^{R_C/R} - 1}{\bar{\gamma}} \right) \quad (41)$$

where  $\gamma(a, x) \triangleq \int_0^x \lambda^{a-1} e^{-\lambda} d\lambda$  is the lower incomplete Gamma function and  $\bar{\gamma} = \frac{1}{R} \frac{\alpha^2}{n_T} \frac{S}{N}$ .

Figure 9 depicts the rate outage probability in percent versus the rate in nats/s/Hz for various STBCs over Rayleigh fading channels at  $S/N = 10\text{dB}$ . Of interest is usually an outage probability of 10%, which means that the channel can support a given rate with a probability of 90%. Clearly, the SISO case performs worst as it supports only 0.7 nats/s/Hz for a 10% outage probability. The half-rate STBCs perform slightly better, achieving gains of approximately 1.05 nats/s/Hz (3 transmit) and 1.15 nats/s/Hz (4 transmit). Interestingly, the full-rate Alamouti scheme does not yield best performance as for the ergodic channel capacity. It achieves 1.3 nats/s/Hz at 10% outage, whereas the 3/4-rate codes yield approximately 1.35 nats/s/Hz (3 antennas) and 1.45 nats/s/Hz (4 antennas).

Figure 10 depicts the rate outage probability in percent versus  $S/N$  in dB for various STBC scenarios over Rayleigh fading channels, required to support a fairly low rate of 1 nat/s/Hz. The same observations as above can be made. The gains of the distributed sensor networks over the SISO communication scenario for an outage of 10% are: 2.5dB (1/2-Rate, 3 transmit antennas), 3.3dB (1/2-Rate, 4 transmit antennas), 4.0dB (Alamouti, 2 transmit antennas), 4.5dB (3/4-Rate, 3

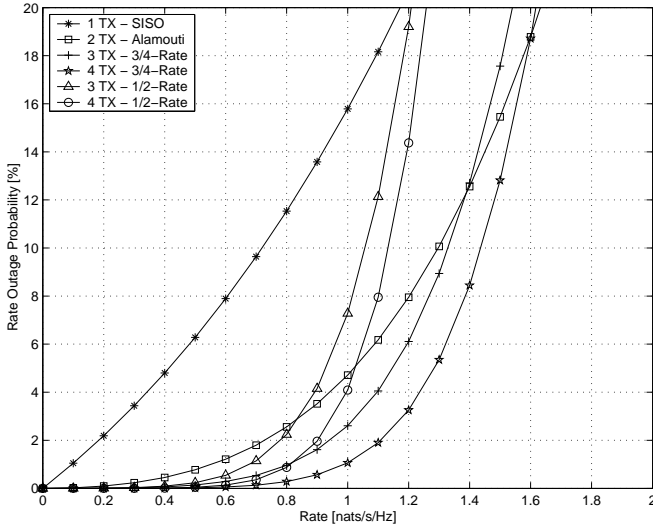


Fig. 9. Outage probability of a given communication rate in percent versus this rate in nats/s/Hz for various STBCs over Rayleigh fading channels;  $S/N = 10\text{dB}$ .

transmit antennas), 5.3dB (3/4-Rate, 4 transmit antennas). It is worth noting that the gains decrease for increasing data rates.

A 5.3dB gain translates to approximately 70% power savings. In contrast to the ergodic channels, it is thus worth deploying distributed sensor networks with more than 2 distributed transmit antennas per sensor tier for non-ergodic channel realisations.

**Unequal Channel Gains.** Computing (40) for the Rayleigh fading channel with the pdf given by (23), one obtains

$$P_{out}(R_C, S, \mathbf{h}) = \sum_{i=1}^{n_T} K_i \cdot \left( 1 - e^{-\frac{e^{R_C/R} - 1}{\bar{\gamma}_i}} \right) \quad (42)$$

where the coefficients  $K_i$  are given by (22) and  $\bar{\gamma}_i = \frac{1}{R} \frac{\alpha_i^2}{n_T} \frac{S}{N}$ . The generic case with repeated  $\gamma_i$  is similarly obtained by

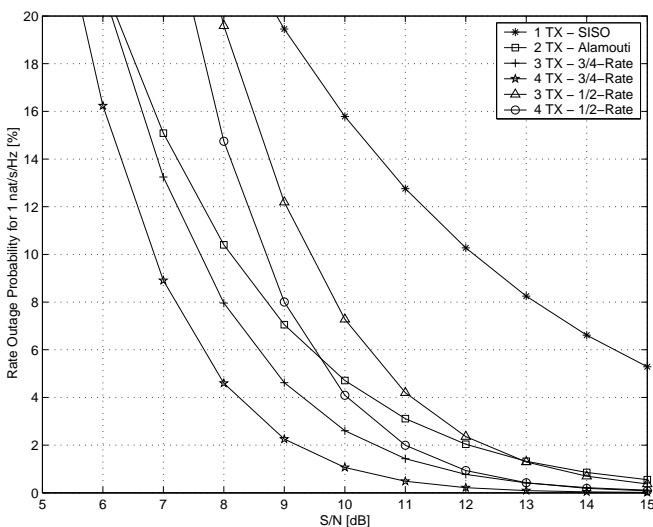


Fig. 10. Outage probability of a given communication rate of 1 nat/s/Hz in percent versus  $S/N$  in dB for various STBC scenarios over Rayleigh fading channels.

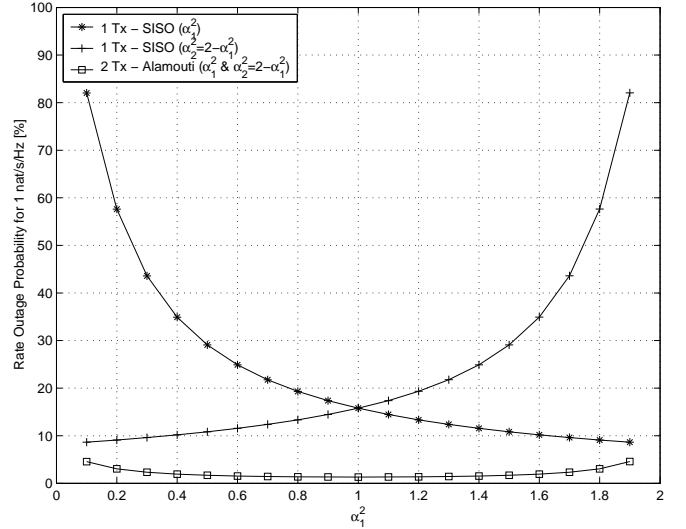


Fig. 11. Outage probability of a given communication rate of 1 nat/s/Hz in percent versus the normalised power in the first link  $\alpha_1^2$  for the distributed Alamouti scheme;  $S/N = 10\text{dB}$ .

utilising the appropriate pdf previously derived.

Figure 11 depicts the rate outage probability in percent versus the normalised power in the first link  $\alpha_1^2$  for the distributed Alamouti scheme with  $S/N = 10\text{dB}$  and a desired communication rate of 1 nat/s/Hz. Again, depicted are the cases where communication happens only over either of the single links, where  $\alpha_2^2 = 2 - \alpha_1^2$ .

Similar to the ergodic case, the outage probability of the distributed scheme is much less dependent on the power of the individual links than the single link schemes. Furthermore, for the chosen system parameters, the distributed scheme can support a rate of 1 nat/s/Hz with an outage probability of less than 10% for any  $\alpha_1^2$ . The single links, however, cannot guarantee this data rate at 10% outage probability for most  $\alpha_1^2$ . It can thus be concluded that in the case of independent shadowing between the nodes, a distributed communication scenario will always bring benefits in terms of power savings or rate outage probabilities when compared to a single link communication scenario.

### B. Orthogonalised MISO - Outage Capacity - Nakagami Fading

**Equal Channel Gains.** Computing (40) for the Nakagami- $m$  fading channel with the pdf given by (34), one obtains

$$P_{out}(R_C, S, \mathbf{h}) = \frac{1}{\Gamma(n_T m)} \gamma \left( n_T m, \frac{e^{R_C/R} - 1}{\bar{\gamma}/m} \right) \quad (43)$$

where  $\bar{\gamma} = \frac{1}{R} \frac{\alpha^2}{n_T} \frac{S}{N}$ . Figure 12 depicts the rate outage probability in percent versus  $S/N$  in dB for the 3/4 rate STBC scenario with 4 distributed transmit antennas over Nakagami fading channels, required to support a rate of 1 nat/s/Hz. The Nakagami fading factor was chosen to be  $m = (1, 2, 4, 6, 8, 10)$ . Increasing the  $m$ -factor from 1 to 10 leads to a power savings of approximately 2.5dB at an outage probability of 10%. Compared to the ergodic capacity, where capacity saturates very fast for increasing  $m$ , this is a notable power gain.

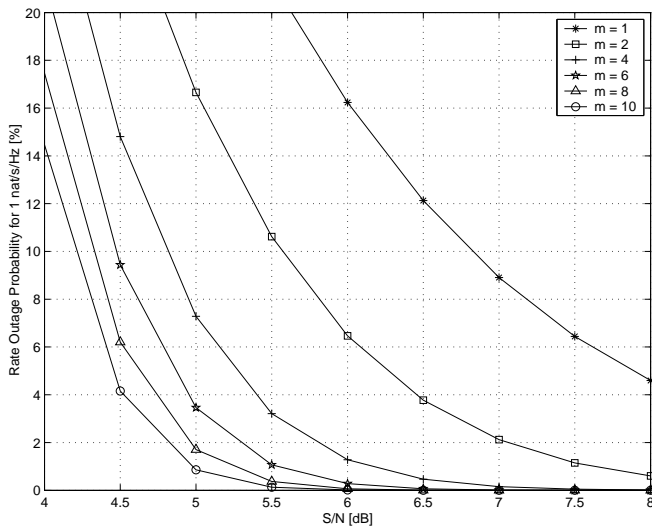


Fig. 12. Outage probability of a given communication rate of 1 nat/s/Hz in percent versus  $S/N$  in dB for the 3/4-rate STBC scenario with 4 distributed transmit antennas over Nakagami fading channels with  $m = (1, 2, 4, 6, 8, 10)$ .

**Unequal Channel Gains.** Finally, the outage probability over different MISO Nakagami distributions can similarly be calculated as

$$P_{out}(R_C, S, \mathbf{h}) = \sum_{i=1}^{n_T} \sum_{j=1}^{m_i} K_{i,j} \cdot \frac{1}{\Gamma(j)} \gamma \left( j, \frac{e^{R_C/R} - 1}{\bar{\gamma}_i/j} \right) \quad (44)$$

where the coefficients  $K_{i,j}$  are found by performing partial fractions on (37) and  $\bar{\gamma}_i = \frac{1}{R} \frac{\alpha_i^2}{n_T} \frac{S}{N}$ .

## V. END-TO-END CAPACITY OF DISTRIBUTED SENSOR NETWORKS

### A. Theoretical Approach

Figure 1 depicts the case of a  $T+1$ -stage distributed sensor network with  $T$  sensor tiers, each acting as a virtual STBC transmit array. The  $i^{\text{th}}$  sensor tier is assumed to be comprised of  $d_i$  sensors, where  $i = (1, \dots, T)$ .

The  $t^{\text{th}}$  stage forms  $d_{t+1}$  MISO channels with  $d_t$  distributed transmit antennas. The  $1^{\text{st}}$  stage is formed by the s-S, which possesses only 1 transmit antenna. The  $(T+1)^{\text{th}}$  stage reaches the t-S and therefore forms only 1 MISO channel. The capacity of each stage is denoted by  $C_{d_t,j}^{(t)}$ , where  $t = (1, \dots, T+1)$  and  $j = (1, \dots, d_t)$ . Since the output of a MISO channel is a fractional input to the consecutive MISO channel, capacity is clearly dominated by the weakest link in the system. Therefore, the end-to-end capacity  $C$  is determined by [41]

$$C = \min \left\{ C_{1,1}^{(1)}, \dots, C_{1,d_1}^{(1)}, C_{d_1,1}^{(2)}, \dots, C_{d_1,d_2}^{(2)}, \dots, C_{d_T,1}^{(T+1)} \right\} \quad (45)$$

To maximise end-to-end capacity, weak MISO links should be excluded; however, this has to be traded-off against the loss in capacity for the consecutive tier. An analytical optimisation approach is very cumbersome, however, possible. The interested reader is referred to approaches suggested in [36], [37], where as well an optimum power and bandwidth allocation is

suggested in dependency of the prevailing channel conditions. The therein suggested approach successfully overcomes the problems associated with the logarithmic capacity Lagrangian, solvable only numerically.

### B. Simulation Assumptions

A multistage distributed sensor network has been simulated with up to 5 stages (i.e. 4 sensor tiers), as depicted in Figure 13. The distance between the source and target sensors has been kept constant with  $d = 100\text{m}$ . This scenario could occur, for instance, in an office building where a remote sensor (s-S) reports to a processing central unit (t-S).

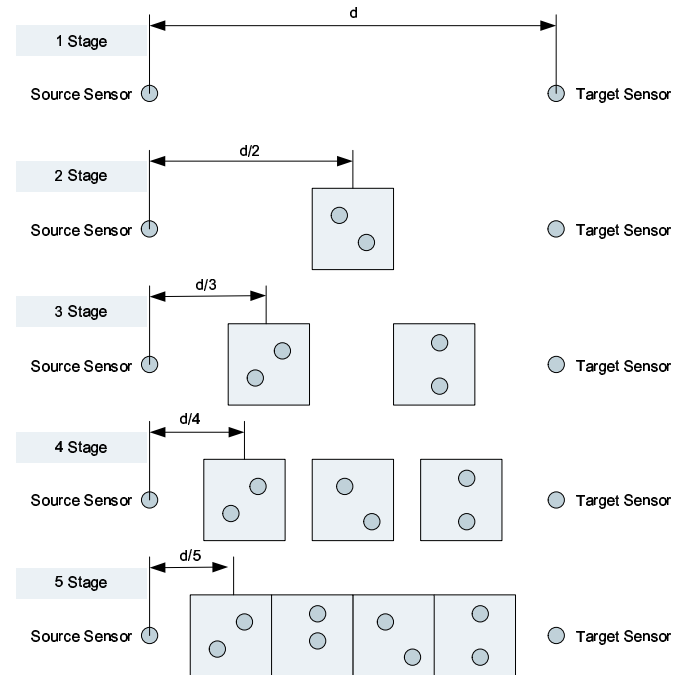


Fig. 13. Multistage distributed sensor network with up to 5 stages (i.e. 4 sensor tiers);  $d = 100\text{m}$ .

The 1-Stage scenario corresponds to a direct link communication scenario over 100m. For the 2-Stage scenario, the first relaying tier is comprised of various distributed sensors which are randomly located in a squared area of the size  $d/5$ . Simulated are only full-rate codes; therefore, only 1 or 2 distributed sensors are uniformly placed into the shaded area.

The distance between the s-S, the centre of the square and the t-S is  $d/2 = 50\text{m}$ . For the 3, 4 and 5-Stage scenarios, the distance between the relaying tiers is chosen to be  $d/3 = 33\text{m}$ ,  $d/4 = 25\text{m}$  and  $d/5 = 20\text{m}$ , respectively. In the 5-Stage scenario, the sensor distribution areas touch each other; this corresponds to the case when sensors are uniformly distributed along the path between the s-S and t-S.

Furthermore, it is assumed that each sensor transmits an average symbol energy of  $E_s = 1\text{nJ}$  measured at 1m distance [42]. The sensor receive noise power spectral density is assumed to be  $N_0 = -140\text{dBm/Hz}$ , i.e. a fairly high noise floor due to cheap manufacturing of the sensor nodes. Thus, the resulting  $S/N = E_s/N_0 = 80\text{dB}$  measured at 1m distance.

Note that an increase in  $E_s$  or decrease in  $N_0$  only leads to a linear shift of subsequent performance curves.

The pathloss model used is the traditional negative exponential pathloss model where the power loss is inversely proportional to  $d^n$ , where  $d$  is the distance and  $n$  the pathloss exponent. For the indoor environment,  $n \approx (3, \dots, 6)$ , where  $n = 3$  corresponds to a lightly and  $n = 6$  to a densely cluttered indoor environment [43].

*C. Capacity of Multistage Distributed Sensor Networks*

**Ergodic Channels without Shadowing.** Figures 14 and 15 relate to a pathloss coefficient of  $n = 3$ . Figures 14 depicts the mean capacity in nats/s/Hz versus the number of stages utilised. At each stage, the network performance with and without STBC is compared, where the deployed STBC is the full-rate Alamouti code. Furthermore, the mean, maximum and minimum capacities have been depicted. Note that there is no fair capacity comparison between the communication scenarios with different stages, as the transmission energy was kept constant per node. If a fair comparison was desired, then the total utilised energy to deliver the information from the s-S to the t-S would have to be equated for all scenarios. Such normalisation was not performed here as the primary aim was to compare distributed with traditional sensor networks.

From Figures 14 it is clear that the capacity of distributed sensor networks is at least as high as for traditional multistage sensor networks. A five-stage distributed sensor network exhibits a 0.25 nats/s/Hz average capacity advantage over the traditional five-stage network. Referring to Figure 2, this leads to a SNR improvement of approximately 1dB. As previously stated, the average capacity is a useful performance measure if the communication channels are ergodic.

Since the positions of the sensor nodes are usually fixed, the channels are not ergodic with respect to the location (mean attenuation); however, the channels are still assumed to be ergodic with respect to the fading statistics. Therefore,

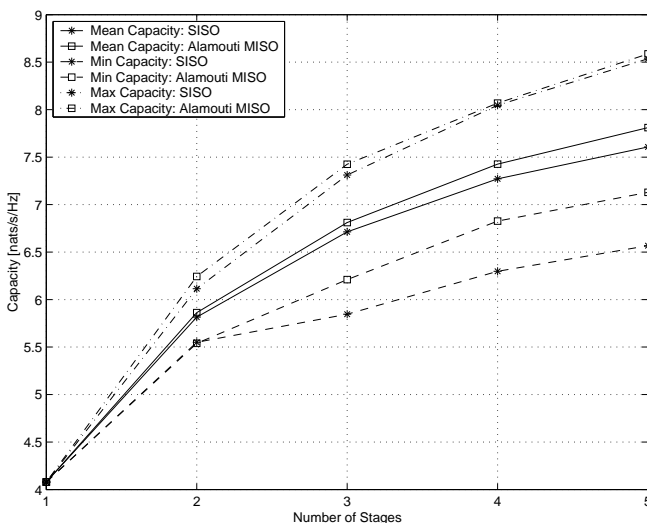


Fig. 14. Normalised minimum, mean and maximum Shannon capacity in nats/s/Hz versus the number of stages utilised; pathloss index  $n = 3$ .

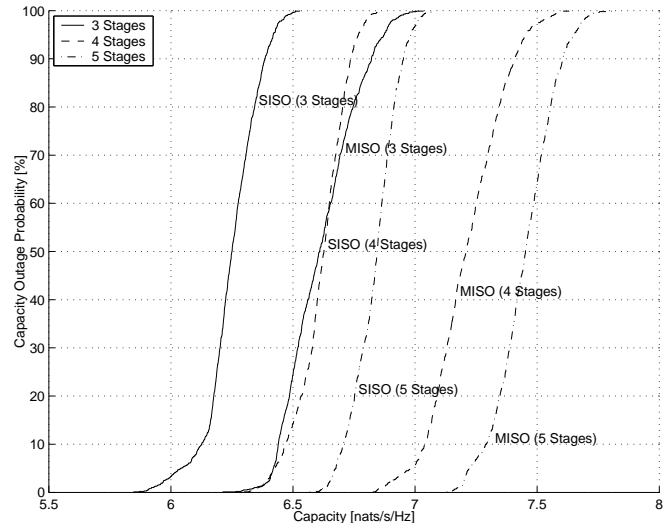


Fig. 15. Outage probability of a given communication rate in percent versus this rate in nats/s/Hz for the 3, 4 and 5-stage single antenna and distributed Alamouti sensor network communication scenario over Rayleigh fading channels without shadowing; pathloss index  $n = 3$ .

Figure 15 depicts the outage probability of the achievable capacity for the chosen uniform sensor distribution.

For the five-stage scenario with uniform sensor distribution at each stage, only 10% of all geometrical sensor distributions cannot support a capacity of 6.7 nats/s/Hz if the traditional SISO scenario is implemented; whereas for the distributed MISO case, all geometrical sensor distributions can support such rate. Only 10% of all five-stage MISO communication scenarios cannot support 7.2 nats/s/Hz. This gives an average capacity advantage of 0.5 nats/s/Hz ( $\equiv 2$ dB) if the respective capacities are to be supported in 90% of all cases.

Equivalently, while the distributed communication scenario can support 7.2 nats/s/Hz at 90% of all cases, the traditional sensor network can support such rate only with close to zero probability (i.e. the outage probability is 100%).

The achieved gains of 2dB translate to a transmit power savings of approximately 40%. This clearly corroborates the advantages of distributed communication over traditional SISO communication scenarios.

**Non-Ergodic Channels with Shadowing.** The outage probability of the attainable rate is obtained here for the case when each link is effected by independent shadowing. For the Monte-Carlo simulations only a small shadowing standard deviation of 0dB was assumed.

Figure 16 depicts the outage probability of the attainable rates versus the rate in nats/s/Hz for the 3, 4 and 5-stage communication scenario. Interestingly, for the chosen sensor distribution, the 3-stage distributed communication scenario does not yield any capacity benefits over the SISO case. Furthermore, the 4-stage distributed case yields only small gains. Finally, when the sensors are densely and uniformly distributed between the s-S and t-S, only then drastic gains can be observed. The latter case corresponds to anticipated high-density sensor network layouts.

The 5-stage distributed sensor network yields a gain of 0.65 nats/s/Hz for an outage probability of 10%. This amounts to a

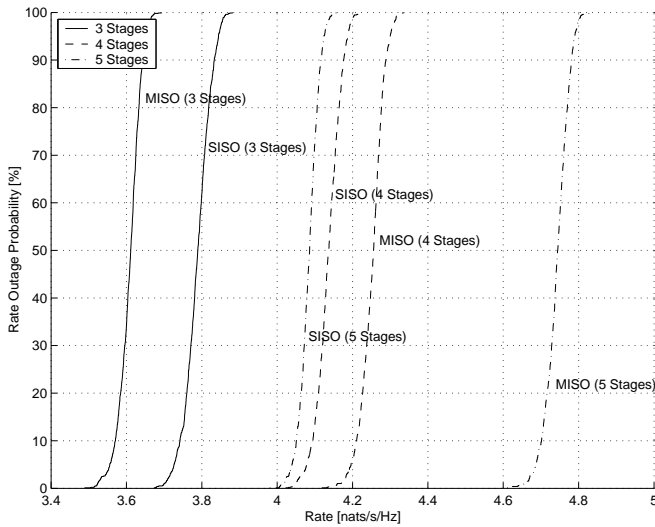


Fig. 16. Outage probability of a given communication rate in percent versus this rate in nats/s/Hz for the 3, 4 and 5-stage single antenna and distributed Alamouti sensor network communication scenario over Rayleigh fading channels with shadowing; pathloss index  $n = 3$  & shadowing standard deviation  $\sigma_S = 0$ dB.

power savings of approximately 3dB, or 50%.

## VI. CONCLUSIONS

This paper derived closed form expressions for the Shannon capacity for sensor networks over distributed ergodic flat-fading Rayleigh and Nakagami channels. Also, derived were the respective outage probabilities in the case of non-ergodic channel realisations.

Space-Time Block Codes (STBCs) allow a simple implementation and are thus suitable for power limited sensor nodes. They are known to orthogonalise the multiple-input-multiple-output (MIMO) channel, which allows an analytical treatment of various capacity and performance problems. Because each sensor node is assumed to possess only 1 antenna element, a distributed network can only realise multiple-input-single-output (MISO) channels. However, the herein exposed analysis is easily extended to the generic MIMO case.

The capacity derivations are based on a closed form expression of the capacity integral, introduced and solved in [37]. It has been utilised to find closed form expressions for the Shannon capacity over ergodic MISO identically distributed flat-fading Rayleigh and Nakagami channels. In the case that each of the wireless links may have a different attenuation or Nakagami  $m$ -factor, closed form capacity expressions are derived by performing partial fractions on the respective moment generating functions (MGF), after which the derivation of the capacity is straightforward. Similarly, the outage probabilities of supportable rates were derived for various configurations.

It has been shown that in the case of ergodic channels, optimum performance is achieved if a distributed Alamouti scheme is deployed. In the case of non-ergodic channels, the outage probability for a desired communication rate is minimised if sporadic 3/4-rate STBCs are utilised with 4 transmit antennas. Gains of up to 5dB could be observed in the case of a distributed sensor deployment, compared to a traditional

single link communication scenario. This clearly demonstrates the benefit of a distributed communication scenario.

Furthermore, Monte-Carlo simulations have been performed to evaluate the average capacity and the associated outage probability for the Alamouti scheme. Again, it could be shown that a distributed deployment generally yields significant performance gains.

Note that sensors cannot operate at Shannon limit due to their limitations on complexity. However, the derived capacity and outage bounds give an indication on the performance of the systems introduced.

## ACKNOWLEDGEMENT

The authors would like to express their gratitude to the anonymous reviewers for their many valuable comments and suggestions.

## APPENDIX

Following the approach exposed in [44, chapter 12], it is proven here that

$$K_{i,j} = \frac{1}{(\nu_i - j)! (-\alpha_i^2)^{\nu_i - j}} \cdot \frac{\partial^{\nu_i - j}}{\partial s^{\nu_i - j}} \left[ \prod_{i'=1, i' \neq i}^g \frac{1}{(1 - s\alpha_{i'}^2)^{\nu_{i'}}} \right]_{s=1/\alpha_i^2} \quad (46)$$

if the partial fractions are applied to (25) which, expanded into its partial fractions, can be expressed as

$$\phi_\lambda(s) = \left[ \frac{K_{1,1}}{(1 - \alpha_1^2 s)^1} + \dots + \frac{K_{1,\nu_1}}{(1 - \alpha_1^2 s)^{\nu_1}} \right] + \dots + \left[ \dots + \frac{K_{g,\nu_g}}{(1 - \alpha_g^2 s)^{\nu_g}} \right] \quad (47)$$

To obtain coefficient  $K_{i,\nu_i}$ , (47) is multiplied with  $(1 - \alpha_i^2 s)^{\nu_i}$  after which  $s$  is set to  $s = 1/\alpha_i^2$  to arrive at  $K_{i,\nu_i} = \prod_{i'=1, i' \neq i}^g \left(1 - \frac{\alpha_{i'}^2}{\alpha_i^2}\right)^{-\nu_{i'}}$ . Furthermore, to obtain coefficient  $K_{i,\nu_i-1}$ , (47) is multiplied with  $(1 - \alpha_i^2 s)^{\nu_i}$ , differentiated w.r.t.  $s$ , after which  $s$  is set to  $s = 1/\alpha_i^2$  to arrive at

$$K_{i,\nu_i-1} = \frac{1}{(-\alpha_i^2)} \frac{\partial}{\partial s} \left[ \prod_{i'=1, i' \neq i}^g \frac{1}{(1 - s\alpha_{i'}^2)^{\nu_{i'}}} \right]_{s=1/\alpha_i^2} \quad (48)$$

Hence, coefficient  $K_{i,1}$  is obtained by multiplying (47) with  $(1 - \alpha_i^2 s)^{\nu_i}$ , differentiated  $(\nu_i - 1)$  times w.r.t.  $s$ , after which  $s$  is set to  $s = 1/\alpha_i^2$  to arrive at

$$K_{i,1} = \frac{1}{(\nu_i - 1)! (-\alpha_i^2)^{\nu_i - 1}} \cdot \frac{\partial^{\nu_i - 1}}{\partial s^{\nu_i - 1}} \left[ \prod_{i'=1, i' \neq i}^g \frac{1}{(1 - s\alpha_{i'}^2)^{\nu_{i'}}} \right]_{s=1/\alpha_i^2}, \quad (49)$$

which concludes the proof.

Note that the  $(\nu_i - j)^{th}$  derivative of  $\prod_{i'=1, i' \neq i}^g (1 - s\alpha_{i'}^2)^{-\nu_{i'}}$  in (46) is easily derived in

closed form. To enhance readability, the following symbolic notation is introduced

$$[\Pi] \triangleq \prod_{i'=1, i' \neq i}^g \frac{1}{(1 - s\alpha_{i'}^2)^{\nu_{i'}}} \quad (50)$$

$$[\Sigma] \triangleq \sum_{i'=1, i' \neq i}^g \frac{\nu_{i'} \alpha_{i'}^2}{1 - s\alpha_{i'}^2} \quad (51)$$

$$[\Sigma^n] \triangleq \sum_{i'=1, i' \neq i}^g \frac{\nu_{i'} (\alpha_{i'}^2)^n}{(1 - s\alpha_{i'}^2)^n} \quad (52)$$

$$\partial^n [\cdot] \triangleq \frac{\partial^n}{\partial s^n} [\cdot] \quad (53)$$

With the introduced notation the following holds

$$\partial[\Sigma^n] = n[\Sigma^{n+1}] \quad (54)$$

$$\partial[\Sigma]^m = m[\Sigma]^{m-1}[\Sigma^2] \quad (55)$$

and generally

$$\partial[\Xi][\Psi] = \partial[\Xi] \cdot [\Psi] + [\Xi] \cdot \partial[\Psi] \quad (56)$$

This allows one finally to rewrite the first order and, inductively, any higher order derivative as

$$\partial[\Pi] = [\Pi][\Sigma] \quad (57)$$

$$\partial^2[\Pi] = \partial[\Pi][\Sigma] \quad (58)$$

$$= \partial[\Pi] \cdot [\Sigma] + [\Pi] \cdot \partial[\Sigma]$$

$$= [\Pi] ([\Sigma]^2 + [\Sigma^2])$$

$$\partial^3[\Pi] = \partial([\Pi] ([\Sigma]^2 + [\Sigma^2])) \quad (59)$$

$$= \partial[\Pi] \cdot ([\Sigma]^2 + [\Sigma^2]) + [\Pi] \cdot \partial([\Sigma]^2 + [\Sigma^2])$$

$$= [\Pi] ([\Sigma]^3 + 3[\Sigma][\Sigma^2] + 2[\Sigma^3])$$

$$\partial^4[\Pi] = [\Pi] ([\Sigma][\Sigma]^3 + 6[\Sigma]^2[\Sigma^2] + 8[\Sigma][\Sigma^3] + 3[\Sigma^2]^2 + 6[\Sigma^4]), \quad (60)$$

etc.

## REFERENCES

- [1] Akyildiz, I.F., W. Su, Y. Sankarasubramaniam, E. Cayirci, "A survey on sensor networks," *IEEE Communications Magazine*, vol. 40 Issue: 8, Aug. 2002 pp. 102 -114
- [2] Rahul C. Shah and Jan Rabaey, "Energy Aware Routing for Low Energy Ad Hoc Sensor Networks", *IEEE Wireless Communications and Networking Conference (WCNC)*, March 17-21, 2002, Orlando, FL.
- [3] Sohrabi, K, Gao, J., Ailawadhi, V, and Pottie, G., "Protocols for self-organization of a wireless sensor network," *IEEE Personal Comm. Magazine*, vol. 7, No. 5, Oct. 2000, pp. 16-27,
- [4] Wireless Integrated Network Sensors, University of California, Los Angeles. Available: <http://www.janet.ucla.edu/WINS>
- [5] J.M. Kahn, R.H. Katz, and K.S.J. Pister, "Next century challenges: Mobile networking for smart dust," *Proc. Mobicom*, 1999, pp. 483-492.
- [6] V. Raghunathan, C. Schurgers, S. Park, and M. B. Srivastava, "Energy Aware Wireless Microsensor Networks", *IEEE Transactions on Signal Processing*, March 2002.
- [7] Shih, E. et al., "Physical layer driven algorithm and protocol design for energy-efficient wireless sensor networks", *Proc. ACM MobiCOM*, July 2001, pp. 272-286.
- [8] Pottie, G.J., and Kaiser, W.J., "Wireless Integrated Network Sensors," *Comm. of the ACM*, vol. 43 No. 5, pp. 51-58, May 2000.
- [9] M. Ahmed, Y-S Tu, and G. Pottie, "Cooperative detection and communication in wireless sensor networks," *38th Allerton Conf. On Comm., Control, and Computing*, Oct 4-6, 2000, pp. 755-764.
- [10] Alec Woo, David E. Culler. "A transmission control scheme for media access in sensor networks", *Proc. ACM MobiCOM*, July 2001, pp. 221-235.
- [11] A. Salhie, and L. Schwiebert, "Power Aware Metrics for Wireless Sensor Networks," *IASTED Conference on Parallel and Distributed Computing and Systems (PDCS 2002) Symposium*, November 2002, pp. 326-331.
- [12] A. Sinha and A. Chandrakasan, "Dynamic Power Management in Wireless Sensor Networks", *IEEE Design and Test of Computers*, March-April 2001, pp. 62-75.
- [13] J.N. Laneman, G.W. Wornell, D.N.C. Tse, "An efficient protocol for realizing cooperative diversity in wireless networks," *Proc. IEEE ISIT*, Washington, D. C., June 2001, p. 294.
- [14] P. Gupta and P. R. Kumar, "Towards and Information Theory of Large Networks: An Achievable Rate Region," *Proc. IEEE Int. Symp. Information Theory (ISIT)*, (Washington DC), p. 150, June 2001.
- [15] A. Reznik, S. Kulkarni, and S. Verdu, "Capacity and Optimal Resource Allocation in the Degraded Gaussian Relay Channel with Multiple Relays," *Proc. Allerton Conf. Communications, Control, and Computing*, (Monticello, IL), Oct. 2002.
- [16] A. Sendonaris, E. Erkip, and B. Aazhang, "User Cooperation Diversity, Part I: System Description," *IEEE Trans. Commun.*, vol. 15, pp. 1927-1938, Nov. 2003.
- [17] A. Sendonaris, E. Erkip, and B. Aazhang, "User Cooperation Diversity, Part II: Implementation Aspects and Performance Analysis," *IEEE Trans. Commun.*, vol. 51, pp. 1939-1948, Nov. 2003.
- [18] J. N. Laneman, D. N. C. Tse, and G. W. Wornell, "Cooperative Diversity in Wireless Networks: Efficient Protocols and Outage Behavior," *IEEE Trans. Inform. Theory*, Accepted for publication.
- [19] J. N. Laneman and G. W. Wornell, "Distributed Space-Time Coded Protocols for Exploiting Cooperative Diversity in Wireless Networks," *IEEE Trans. Inform. Theory*, vol. 49, pp. 2415-2525, Oct. 2003.
- [20] Y. Tang and M.C. Valenti, "Coded transmit macrodiversity: Block space-time codes over distributed antennas," *Proc. IEEE Vehicular Tech. Conf. (VTC)*, (Rhodes, Greece), May 2001, pp. 1435-1438.
- [21] T. E. Hunter and A. Nosratinia, "Cooperation Diversity through Coding," *Proc. IEEE Int. Symp. Information Theory (ISIT)*, (Lausanne, Switzerland), p. 220, July 2002.
- [22] A. Stefanov, E. Erkip, "On the performance analysis of cooperative space-time coded systems," *Wireless Communications and Networking*, 2003. WCNC 2003. 2003 IEEE, Vol. 2, March 2003, pp. 729-734, vol.2
- [23] P.A. Anghel, G. Leus, M. Kavehl, "Multi-user space-time coding in cooperative networks," *Acoustics, Speech, and Signal Processing*, 2003. Proceedings. (ICASSP '03). 2003 IEEE International Conference, Vol. 4, April 2003, pp. 73-6, vol. 4
- [24] Y. Hua, Y. Mei, Y. Chang, "Wireless antennas making wireless communications perform like wireline communications," *IEEE Topical Conference on Wireless Communication Technology*, pp. 1-27, Honolulu, Hawaii, Oct 15-17, 2003.
- [25] A. Stefanov, E. Erkip, "Cooperative Coding for Wireless Networks," *4th IEEE Conf. on Mobile and Wireless Communication Networks*, September, 2002.
- [26] S. M. Alamouti, "A simple transmit diversity technique for wireless communications", *IEEE Journal on selected areas in communications*, vol. 16, No. 8, Oct. 1998.
- [27] V. Tarokh, H. Jafarkhani, A. Calderbank, "Space-Time Block Codes from Orthogonal Design", *IEEE Trans. Inform. Theory*, Vol 45, No. 5, July 1999, pp. 1456-1466.
- [28] V. Tarokh, H. Jafarkhani, and A. R. Calderbank, "Space-time block coding for wireless communications: Performance results", *IEEE Journal on selected areas in communications*, vol. 17, No. 3, Mar. 1999, pp. 451-460.
- [29] V. Tarokh, N. Seshadri, A. Calderbank, "Space Time Codes for high data rate wireless communication: performance criterion and code construction", *IEEE Trans. Inform. Theory*, Vol 44, No. 2, March 1998, pp. 744-765.
- [30] G.J. Foschini, "Layered Space-Time Architecture for Wireless Communication in a Fading Environment When Using Multi-Element Antennas", *Bell Labs Technical Journal*, Vol. 1, No. 2, Autumn 1996, pp 41-59.
- [31] H. Shin and J.H. Lee, "Exact symbol error probability of orthogonal space-time block codes," *Proc. of the IEEE Globecom*, Taipei, Taiwan, Nov. 17-21, pp.1547-1552, 2002.
- [32] R. U. Nabar, H. Bölcskei, and A. J. Paulraj, "Outage performance of space-time block codes for generalized MIMO channels," *IEEE Trans. Information Theory*, Mar. 2002, submitted.
- [33] E.G. Larsson, P. Stoica, *Space-Time Block Coding for Wireless Communications*, Cambridge University Press, 2003.

- [34] M. Dohler, F. Said, A. Ghorashi, H. Aghvami, "Improvements in or Relating to Electronic Data Communication Systems", Publication No. WO 03/003672, priority date 28 June 2001.
- [35] M. Dohler, A. Gkelias, H. Aghvami, "2-Hop Distributed MIMO Communication System", *IEEE Electronics Letters*, vol. 39, no. 18, Sept. 2003, pp.1350-1351.
- [36] M. Dohler, A. Gkelias, H. Aghvami, "A Resource Allocation Strategy for Distributed MIMO Multi-Hop Communication Systems", *IEEE Communications Letter*, vol.8, no.2, February 2004, pp. 99-101.
- [37] M. Dohler, *Virtual Antenna Arrays*, PhD Thesis, University of London, London, 2003.
- [38] J. Proakis, *Digital communications*, McGraw Hill, Fourth edition.
- [39] E. Telatar, "Capacity of multi-antenna Gaussian channels", *European Transactions on Telecommunications*, Vol. 10, No. 6, Nov./Dec. 1999, pp. 585-595.
- [40] M.K. Simon, M-S. Alouini, *Digital Communication over Fading Channels*, John Wiley & Sons, Inc., Wiley Series in Telecommunications and Signal Processing, 2000.
- [41] T. Cover, J.A. Thomas, *Elements of Information Theory*, John Wiley & Sons, Inc., 1991.
- [42] Twan Basten, Luca Benini, Anantha Chandrakasan, Menno Lindwer, Jie Liu, Rex Min, Feng Zhao, "Scaling into Ambient Intelligence", 2003 Design, Automation, and Test in Europe, Munich, Germany, March 2003.
- [43] R. Vaughan, J.B. Andersen, "Channels, Propagation and antennas for mobile communications", *IEE*, Electromagnetic Wave Series, 2003.
- [44] J.W. Nilsson, S.A. Ridel, *Electric Circuits*, Prentice-Hall International, Inc., sixth edition, 2000.



**A. Hamid Aghvami** joined the academic staff at King's College, London in 1984. In 1989 he was promoted to Reader and Professor in Telecommunications Engineering in 1992. He is presently the Director of the Centre for Telecommunications Research at King's. Professor Aghvami carries out consulting work on Digital Radio Communications Systems for both British and International companies. He has published over 300 technical papers and given invited talks all over the world on various aspects of Personal and Mobile Radio Communications as well as giving courses on the subject worldwide. He was Visiting Professor at NTT Radio Communication Systems Laboratories in 1990 and Senior Research Fellow at BT Laboratories in 1998-1999. He is currently Executive Advisor to Wireless Facilities Inc., USA and Managing Director of Wireless Multimedia Communications LTD (his own consultancy company). He leads an active research team working on numerous mobile and personal communications projects for third and fourth generation systems, these projects are supported both by the government and industry. He is a distinguished lecturer and a member of the Board of Governors of the IEEE Communications Society. He has been member, Chairman, Vice-Chairman of the technical programme and organising committees of a large number of international conferences. He is also founder of the International Conference on Personal Indoor and Mobile Radio Communications (PIMRC). He is a fellow of the Royal Academy of Engineering, IEE and IEEE.



**Mischa Dohler** obtained his MSc degree in Telecommunications from King's College London in 1999, and his Diploma in Electrical Engineering from Dresden University of Technology, Germany, in 2000. He has been lecturer at the Centre for Telecommunications Research, King's College London, until June 2005. He is now in the R&D department of France Télécom working on embedded and future communication systems. Prior to Telecommunications, he studied Physics in Moscow. He has won various competitions in Mathematics and Physics,

and participated in the 3rd round of the International Physics Olympics for Germany. He has published numerous research papers and holds six patents. He is a member of the IEEE, has been the Student Representative of the IEEE UKRI Section and a member of the Student Activity Committee of IEEE Region 8. He has also been the London Technology Network Business Fellow for King's College London.



**Athanasios Gkelias** graduated from Aristotle University of Thessaloniki, Greece (AUTH), Department of Electrical and Computer Engineering, in 2000. In 2001 he obtained his MSc degree in Telecommunications from King's College, University of London, England. He is currently working towards his Ph.D. degree at the Centre for Telecommunication Research, King's College London. His research interest lies in the area of ad-hoc and sensor networks, particularly interested in performance analysis and design of medium access control

protocols.